Title

Solvent Control of Chemical Identity Can Change Photodissociation into Photoisomerization

Journal

The Journal of Physical Chemistry Letters, 13(34)

ISSN

1948-7185

Authors

Vong, Andy
Mei, Kenneth J
Widmer, Devon R
et al.

Publication Date

2022-09-01

DOI

10.1021/acs.jpclett.2c01955

Peer reviewed

THE JOURNAL OF PHYSICAL CHEMISTRY LETTERS
A JOURNAL OF THE AMERICAN CHEMICAL SOCIETY

pubs.acs.org/JPCL

Letter

Solvent Control of Chemical Identity Can Change Photodissociation into Photoisomerization

Andy Vong, Kenneth J. Mei, Devon R. Widmer, and Benjamin J. Schwartz*

Cite This: J. Phys. Chem. Lett. 2022, 13, 7931−7938

Read Online

ACCESS | Metrics & More | Article Recommendations | Supporting Information

ABSTRACT: In solution-phase chemistry, the solvent is often considered to be merely a medium that allows reacting solutes to encounter each other. In this work, however, we show that moderate locally specific solute−solvent interactions can affect not only the nature of the solute but also the types of reactive chemistry. We use quantum simulation methods to explore how solvent participation in solute chemical identity alters reactions involving the breaking of chemical bonds. In particular, we explore the photoexcitation dynamics of Na_2^+ dissolved in liquid tetrahydrofuran. In the gas phase, excitation of Na_2^+ directly leads to dissociation, but in solution, photoexcitation leads to an isomerization reaction involving rearrangement of the first-shell solvent molecules; this isomerization must go to completion before the solute can dissociate. Despite the complexity, the solution-phase reaction dynamics can be captured by a two-dimensional energy surface where one dimension involves only the isomerization of the first-shell solvent molecules.

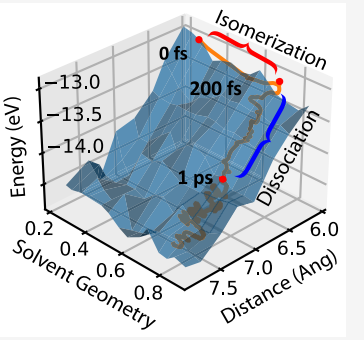

Most chemical reactions take place in solution, where the solvent is typically viewed as a background medium for reacting solute molecules to encounter one another via diffusion. Of course, for a few special cases, such as solvated electrons[1] and charge-transfer-to-solvent transitions,[2,3] solvents can help to create electronic states that otherwise would not exist if the solutes were in the gas phase. And in electron transfer and related reactions, solvent reorganization is the primary driving force to move charge from the donor to the acceptor and thus determines the reaction rate.[4−9]

In addition to the special cases where reactions cannot occur without solvent mediation, the presence of solvent molecules can also strongly alter our gas-phase-like picture of solution-phase chemistry: solvent molecules can do much more than act as a reactive medium. For example, first-shell solvent molecules can "cage" the products of photodissociation reactions, inhibiting separation of the photofragments and promoting recombination.[10−14] Additionally, photoreaction pathways and photofragment relaxation time scales can differ depending on solvent polarity[15−17] or viscosity.[18] Moreover, solvent interactions can alter the potential energy surface on which reactions take place, changing them significantly from what they were for an isolated gas-phase solute.[19−28] Previously, we have shown that Pauli repulsion interactions from surrounding solvent molecules can compress a solute's bonding electrons, raising a solute's bond vibrational frequency.[29] We have also shown that modest locally specific solute−solvent interactions, with energetics similar to those of a hydrogen bond, can change the chemical identity of a solute.[30,31] In such cases, the chemical species must be thought of as a solute−solvent complex rather than a gas-phase solute perturbed by solvent interactions.[30,31]

In this work, we use quantum simulation methods to examine how solvent-induced changes in chemical identity affect the breaking of chemical bonds. In particular, we show that for a diatomic solute that normally undergoes a photodissociation reaction in the gas phase, the chemistry following photoexcitation in solution is entirely different: the solution-phase dynamics involves a two-step process whose first step is best described as a photoisomerization reaction involving solvent rearrangement, followed by a second quasi-dissociative step that can take place only after the solvent isomerization is complete. Because rearrangement of the solvent molecules rather than the separation of solute photofragments dominate the early time dynamics, the solution-phase reaction needs to be described by a two-dimensional potential energy surface involving collective motion of the first-shell solvent molecules rather than the simpler one-dimensional potential energy curves that describe the gas-phase photoreactivity. The results indicate that the solvent can play an intimate role in chemical reactions involving bond breaking or formation, potentially requiring a whole new formalism beyond what is typically used for solution-phase reactivity.

The system we choose to study in this work is the Na_2^+ molecule dissolved in liquid tetrahydrofuran (THF), which we

Received: June 24, 2022
Accepted: August 10, 2022

https://doi.org/10.1021/acs.jpclett.2c01955
J. Phys. Chem. Lett. 2022, 13, 7931−7938

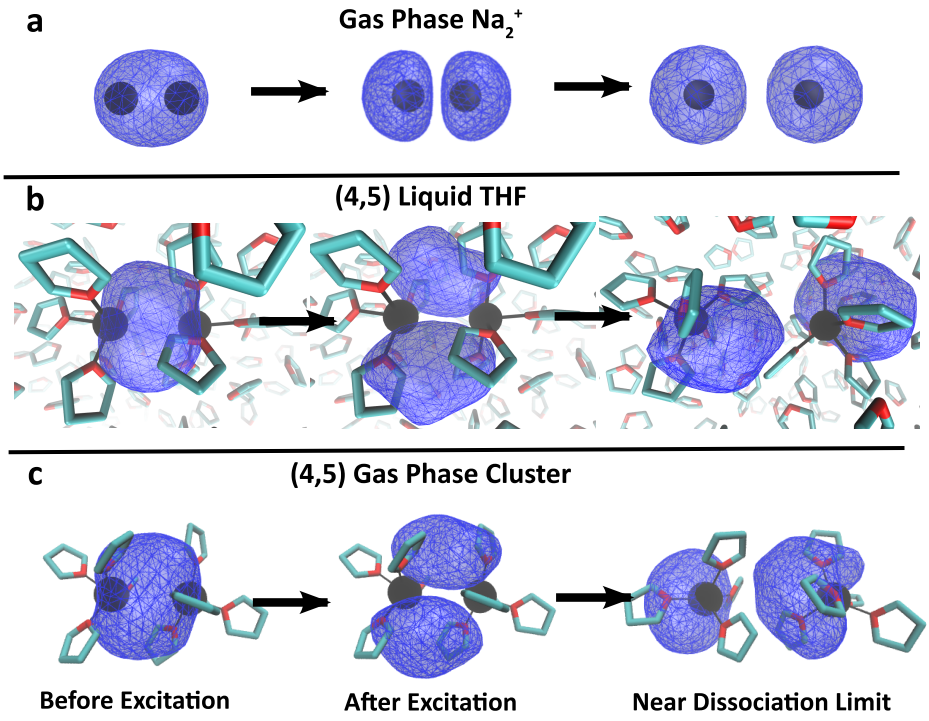

Figure 1. Simulation snapshots of the excited-state electron density for Na_2^+ in different environments: (a) the gas phase; (b) in liquid THF; (c) as a gas-phase $Na(THF)_4$−$Na(THF)_5^+$ solvated cluster. In each panel, the left-most image displays a snapshot of the Na_2^+ species in its ground-state equilibrium, the center image shows the electron density in the Franck−Condon region immediately after photoexcitation, and the right-most image shows the excited-state electron density after the photofragments have separated to a distance of ∼8 Å. The Na^+ cores are plotted as black spheres, and THF solvent molecules are plotted as turquoise sticks with red oxygen atoms. Dative bonds are shown as thin black lines connecting THF oxygen sites and Na^+. The gas-phase Na_2^+ bonding electron density resembles a σ^* MO immediately after photoexcitation. In the presence of datively bonded THF, however, the Franck−Condon excited-state bonding electron density resembles a π MO, whose node reorients to a σ^* orientation by the dissociation limit.

simulate using mixed quantum/classical (MQC) molecular dynamics (MD). The Na^+ solute cores and THF solvent molecules are treated classically, while the valence bonding electron is treated quantum mechanically. We simulate photoexcitation of the solute by taking uncorrelated equilibrium configurations of the ground-state system and placing the bonding electron onto its first excited state at time zero, then propagating dynamics adiabatically to generate a nonequilibrium ensemble of 20 trajectories. We chose this system because it is readily amenable to study via MQC MD: the electronic structure of gas-phase Na_2^+ is fairly easy to describe because of the relative lack of exchange and correlation contributions between the valence bonding electron and the core electrons,[32] and the necessary electron−Na^+ core and electron−THF pseudopotentials[33] have already been developed and thoroughly benchmarked.[34−37] The methods we employ here are similar to those in our previous work,[21,30,31] and they reproduce the gas-phase quantum chemistry of Na_2^+[32,34] and experimental properties of Na^+:solvated electron tight contact pairs in liquid THF quite well.[37,38] Further details are given in Methods and the Supporting Information.

In the following discussion we will show that the character of the bonding electron will change from π-like to σ^*-like. For systems where the change in bond length can be significant, such as ours, it is possible that the electronic character of the excited states might change as a result of diabatic crossing, for which the use of adiabatic dynamics would not be appropriate. However, our analysis shows that the change in electronic character following photoexcitation of our system is driven adiabatically by solvent rearrangement. A detailed discussion of why adiabatic dynamics are appropriate for our study is given in the Supporting Information.

As a reference point for understanding solvent effects on chemical bond-breaking, we begin our analysis by studying the behavior of the photoexcited Na_2^+ solute in the gas phase. Figure 1a shows snapshots of the bonding electron's charge density for the solute in the ground state before excitation (left), in the Franck−Condon region immediately following excitation (center), and when the fragments have separated to a distance of 8 Å (right). The ground and Franck−Condon excited-state charge densities clearly resemble bonding σ and antibonding σ^* molecular orbitals, respectively, with the nodal plane of the excited-state wave function oriented perpendicular to the bond axis. As the molecule separates, half the bonding electron is associated with each Na^+ core, as there is nothing in the gas phase to break the symmetry to localize the electron and create the eventual Na^0 + Na^+ photoproducts. We[21,39] and Gervais and co-workers[14,40] have also explored how Na_2^+ behaves in Ar following photoexcitation. Gervais and co-workers also noticed an inversion of electronic structure character with Li_2^+ in Ne_n clusters, although from diabatic crossing.[20]

In liquid THF, however, the solvent forms dative bonds to the solute,[37] which changes the solute chemical identity.[30] For Na_2^+ in liquid THF, two new chemical species are formed, consisting of $Na(THF)_4$−$Na(THF)_5^+$ and $Na(THF)_5$−$Na(THF)_5^+$ complexes, which we will refer to as (4,5) and (5,5), respectively, for brevity. We have previously argued that these complexes are separate molecules (with a ∼6 k_BT barrier for

https://doi.org/10.1021/acs.jpclett.2c01955
J. Phys. Chem. Lett. 2022, 13, 7931−7938

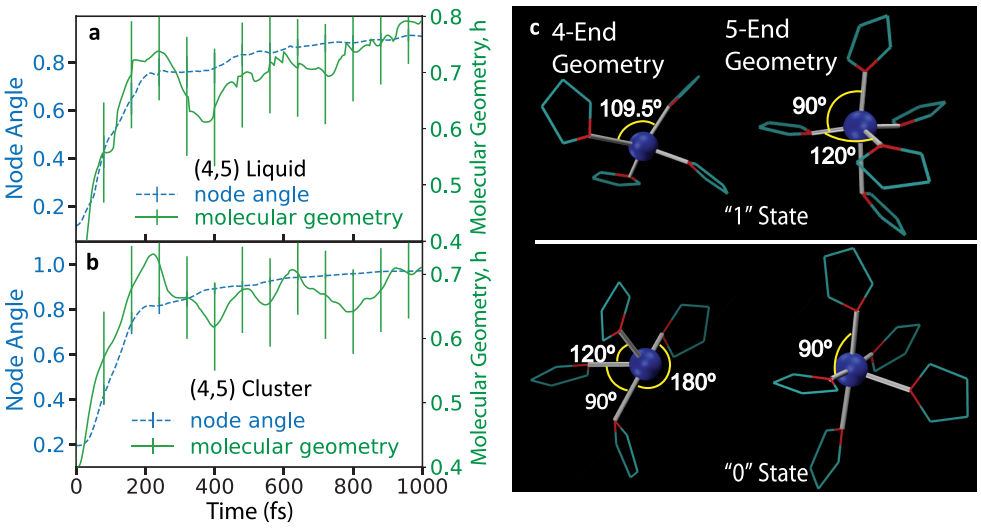

Figure 2. Nonequilibrium ensemble average dynamics of the molecular geometry, h (green curves), and node angle (dashed blue curves) of the (4,5) species following photoexcitation. Panel a shows the molecular geometry and node angle evolution for the (4,5) complex in liquid THF, while panel b shows the same for the (4,5) gas-phase cluster. In both cases, there is a significant change in the molecular geometry over the first ∼200 fs that is correlated with a change in the node angle. Panel c illustrates the ideal molecular geometry states of both the 4-coordinate and 5-coordinate ends of the (4,5) complex with h = 0 equating to a seesaw/square pyramidal state and h = 1 equating to a tetrahedral/trigonal bipyramidal state. Error bars represent the standard error.

interconversion between them) with distinct Na^+-Na^+ bond lengths, vibrational frequencies, and electronic absorption spectra.[31] Here, we focus on the chemistry following photoexcitation of the (4,5) species for conciseness, but a similar analysis and conclusions for photoexcitation of the (5,5) complex can be found in the Supporting Information.

The change in chemical identity from gas-phase Na_2^+ to a (4,5) (or (5,5)) solvated complex completely changes the electronic structure of this species,[30,31] as can be seen in Figure 1b. Due to Pauli repulsion of the datively bound THF molecules, the bonding electron has its excited-state node oriented parallel to the Na^+-Na^+ bond axis, similar to the structure of a π bonding molecular orbital (center). As the Na^+-Na^+ distance lengthens, the electron density shifts so that the node now lies perpendicular to the bond axis, picking up σ^* character (right; see also the movie of this process included in the Supporting Information).[21] Because of the differences in electron density between panels a and b of Figure 1, photoexcitation of Na_2^+ in liquid THF, where dative bonds with the solvent cause changes in the chemical identity of the solute, cannot be thought of as simply a gas-phase Na_2^+ photodissociation reaction slightly perturbed by the solvent.

In Figure 1c, we show what happens following photoexcitation of a (4,5) Na_2^+/THF complex as a gas-phase cluster, removing the effect of the bulk solvent. The excited-state relaxation process in this case is similar to what occurs in the full liquid phase, where the bonding electron initially has π character but transitions to have more σ^* character by 8 Å. This verifies that the datively bound THF molecules are important participants in this photoexcitation reaction, confirming that the proper chemical identity is a complex that includes the datively bound THFs rather than a solvent-perturbed Na_2^+. A comparison between panels b and c of Figure 1, however, shows that photoexcitation of (4,5) in solution can be thought of as similar to that of the gas-phase (4,5) complex with minor perturbations, emphasizing that including the datively bound solvents as part of the solute is necessary to understand this condensed-phase photoreaction.

The snapshots seen in Figure 1 lead to an obvious question: what causes the excited-state bonding electron to change its character from π-like to σ^*-like? The answer lies in the specific datively bonded solvent molecular geometry and how this geometry evolves following photoexcitation. For the 4-coordinated end of the (4,5) complex, the solvents are initially arranged in a seesaw configuration and evolve into a more tetrahedral configuration after photoexcitation and subsequent relaxation. For the 5-coordinated end of the (4,5) complex, we see square pyramidal and trigonal bipyramidal configurations before and after photoexcitation, respectively. To track the dynamics of these local solvent geometry changes, we define an order parameter, $h(t)$, based on the interior angles of the coordinating THFs at each end of the (4,5) complex. The $h(t)$ function is constructed to have a value of 0 when the local geometry is seesaw/square pyramid and a value of 1 when the local geometry is tetrahedral/trigonal bipyramid. Details of how $h(t)$ was constructed are given in Methods.

Figure 2 shows the connection between the molecular geometry, $h(t)$, of the (4,5) complex (green curves) and the change from π-like to σ^*-like character, via the angle of the node in the excited-state wave function relative to the Na^+-Na^+ bond axis (blue curves), for the first picosecond following excitation. The node angle is calculated by taking the dot product of the ground-to-first-excited-state transition dipole moment with a unit vector along the Na^+-Na^+ bond axis, so that a value of 0 results when the nodal plane is parallel to the bond axis (π-like) and a value of 1 means that the nodal plane is perpendicular to the bond axis (σ^*-like). The data show that the rotation of the excited-state node from parallel to perpendicular occurs during the same ∼200 fs period following excitation as the coordinating THFs change their geometry from a seesaw/square pyramid to a tetrahedral/trigonal bipyramid configuration. In other words, after photoexcitation, the motions of the datively bound solvent molecules are directly tied to the rotation of the node in the bonding electron's wave function. Since the distance between the two photofragments does not change during this solvent rearrange-

https://doi.org/10.1021/acs.jpclett.2c01955
J. Phys. Chem. Lett. 2022, 13, 7931−7938

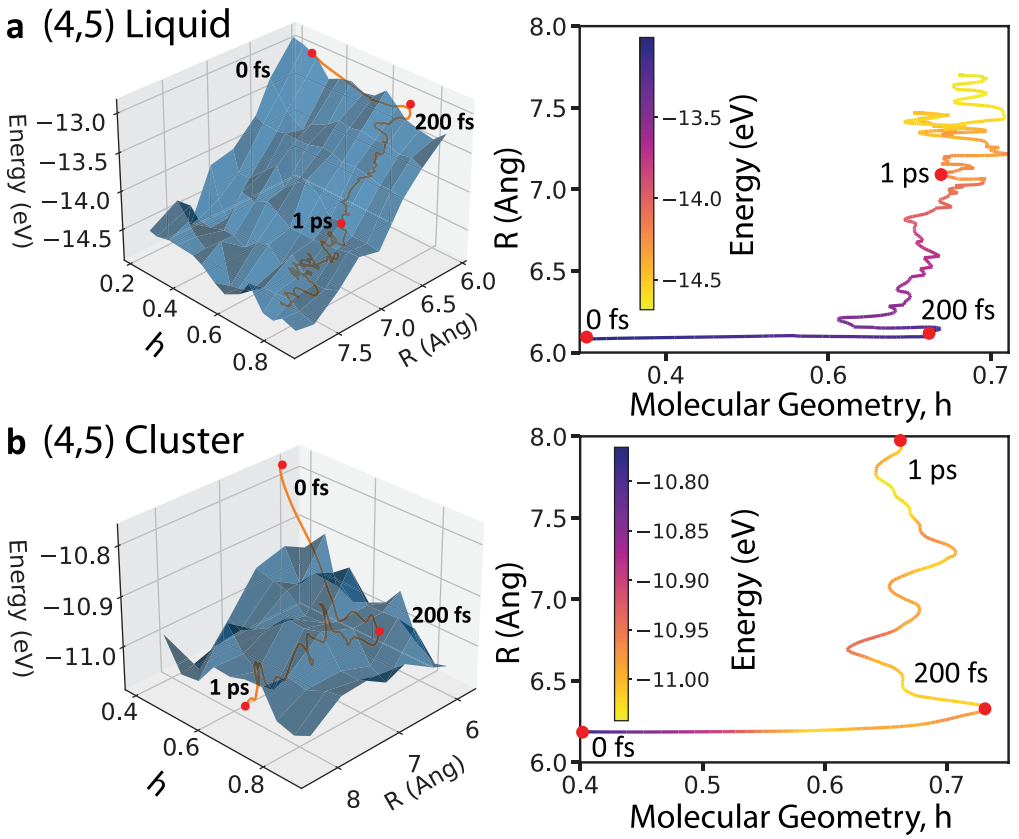

Figure 3. Two-dimensional energy surfaces (shown in blue in the left diagrams) with axes representing the datively bonded solvent geometry, *h*, and the photofragment distance separation, *R*, for the nonequilibrium dynamics following photoexcitation of a (4,5) Na_2^+/THF complex (a) in liquid THF and (b) as a gas-phase cluster. The right diagrams show the same nonequilibrium average trajectory from a "top-down" view with the color used to indicate the value of the energy. The time following photoexcitation is shown at a few select points. Clearly, the first ∼200 fs of the motion out of the Franck−Condon region is entirely along *h*, effectively a photoisomerization reaction that is associated with a ∼ 200 meV drop in energy. Only after the isomerization is complete can the system begin to move along the *R* dissociative coordinate. Dissociation of the gas-phase cluster in panel b is driven by only a ∼100 meV energy loss, while that of the (4,5) complex in the liquid in panel a is accompanied by nearly a 1 eV energy loss due to a change in chemical identity as the reaction occurs (cf. Figure 4).

ment, as discussed further below, we refer to the dynamics during this ∼200 fs window as a photoisomerization process.

The fact that the initial photoexcitation produces an excited-state wave function with more π character than σ^* character suggests that there is little driving force to separate the Na^+ ions in the Franck−Condon region: in other words, the presence of the datively bonded THF solvents means that photoexcitation is not initially dissociative.[21] Yet, if trajectories are run for a sufficiently long time, i.e., a time much longer than necessary for the gas-phase photodissociation reaction, the Na^+ ions in liquid THF eventually do separate. To understand this later-time separation and include the fact that the datively bonded solvent molecules are part of the identity of the molecule,[30,31] we define a dissociation parameter, *R*, based on the distance between the centers of mass of the $Na(THF)_4^+$ and $Na(THF)_5^+$ photofragments. What we will show next is that *h* and *R* represent effectively orthogonal parameters that are capable of describing the excited-state dynamics of (4,5) complexes in either liquid THF or the gas phase.

The left side of Figure 3 shows two-dimensional energy surfaces for the photoexcitation of (4,5) in liquid THF (panel a) and for the (4,5) gas-phase complex (panel b), where one axis is the datively bonded solvent molecular geometry, *h*, and the other is the distance between photofragment centers of mass (COM), *R*. The specifics of how these surfaces were generated are included in Methods. Briefly, these surfaces show the enthalpic contribution to the dynamics calculated directly from the solute potential energies during the nonequilibrium trajectories; thus, they are not free energy surfaces as they do not include any entropic contributions. An accurate representation of the free energy landscape would require transition path or importance sampling methods, which would have been prohibitive given the expense computational associated with the quantum mechanically determined trajectories. Fortunately, it appears that an enthalpy representation is sufficient for our analysis.[41−43] Superimposed on the energy surfaces are orange curves showing the time-averaged behavior of the nonequilibrium ensemble. The right side of Figure 3 shows the same 2-D nonequilibrium average behavior from a "top-down" view, where the energy change is shown via the color of the curve. The time along the nonequilibrium average trajectory is labeled at a few select points in both sets of plots.

At the time of photoexcitation, Figure 3 shows that the average equilibrium configuration of the (4,5) complex has a value of $R \approx 6$ Å and $h \approx 0.4$, indicating a geometry that is closer to seesaw/square pyramid. Immediately following photoexcitation, the (4,5) complex in liquid THF (Figure 3a) spends the first ∼200 fs moving solely along the molecular

https://doi.org/10.1021/acs.jpclett.2c01955
J. Phys. Chem. Lett. 2022, 13, 7931−7938

geometry coordinate, with the datively bonded THFs isomerizing to achieve a more tetrahedral/trigonal bipyramid structure (h = 0.8), a process that is driven by an energy drop of ∼200 meV. The energy surface, which is calculated using only the enthalpy, does not show a clear barrier that forces motion along only the molecular geometry coordinate, but an entropic barrier must be present since dissociative motion does not take place until after the isomerization is complete. Only after the isomerization is complete does the system begin to move along the COM-to-COM distance coordinate (accompanied by fluctuations along the geometry coordinate), which leads to a roughly 1 eV additional energy drop. The velocity of motion along the R distance coordinate (compare Figure 4) is much slower than for a bare gas-phase Na_2^+ molecule, so we refer to this separation as being only weakly dissociative. For comparison, the photodissociation reaction of bare gas-phase Na_2^+ has the fragments reaching a distance of 8 Å by ∼140 fs.

For photoexcitation of a gas-phase (4,5) complex (Figure 3b), the first ∼200 fs of dynamics after excitation is nearly identical to that seen in solution, with motion solely along the molecular geometry axis and an associated energy drop of ∼200 meV. Once the isomerization is complete, the system then moves slowly along the R coordinate, but the energy drop along this coordinate is now only ∼100 meV instead of nearly 1 eV. The net conclusion from Figure 3 is that once we account for the fact that the solvent is part of the chemical identity of the molecule, the energy surface to describe photoexcitation is two-dimensional: photoexcitation results in a two-step, sequential process where the first step involves solely isomerization of the datively bonded THFs. This means that carefully considering the chemical identity and choosing the correct reaction coordinates are critical for understanding solution-phase photexcitation reactions: if one were to think of the species as Na_2^+ dissolved in THF without explicitly considering the solvent, there would be no easily constructed potential energy surface that could readily explain the excited-state dynamics of this species.[21]

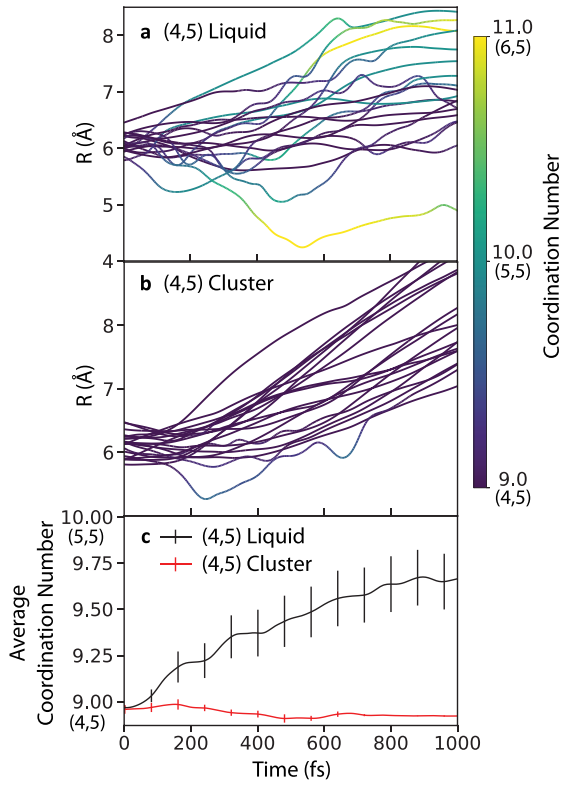

Figure 4. Plot of (4,5) Na_2^+/THF complex fragment distance coordinate, R, following nonequilibrium photoexcitation, with the color representing the total coordination number of datively bonded THFs in (a) liquid THF and (b) as a gas-phase cluster. As the R coordinate for the (4,5) complex in liquid THF increases, panel a shows that the total THF coordination number increases, indicating a change in chemical identity to (5,5) and in a few cases, to (5,6). In panel b, the (4,5) cluster coordination number cannot change with time because there are no additional solvent molecules with which to coordinate. Panel c plots the nonequilibrium ensemble average of the THF coordination number for the initially-(4,5) complex in the liquid (black curve) and as a gas-phase cluster (red curve). The additional complexation in the liquid is what leads to the extra dissociative driving force seen in Figure 3a. The error bars shown in panel c are for the standard error.

Figure 3 also leaves us with an interesting puzzle: why is the energy drop along the R coordinate nearly an order of magnitude larger for the (4,5) complex in solution than that for the same complex in the gas phase? The two sets of simulations differ only in the presence of additional classical solvent molecules, so somehow the presence of extra THF molecules leads to additional relaxation, but only after the initial photoisomerization reaction is complete. To understand where this additional energy relaxation comes from, in Figure 4 we plot the photofragment separation, R, and the total solvent coordination number of the complex (on a color scale) against time for the initially-(4,5) complex in both liquid THF (panel a) and as a gas-phase complex (panel b). The THF coordination number is calculated using a counting coordinate[30,31,37,38] based on the distance of the datively bonded THF oxygen atom from the Na^+ core, as detailed in Methods.

Figure 4b shows that the gas-phase (4,5) complex does not change its THF coordination with time, which makes sense given that the complex is isolated in the gas phase. The situation is quite different, however, when the (4,5) complex is photoexcited in liquid THF. Figure 4a shows that once the isomerization is complete, THF molecules from the surrounding solvent can begin to datively coordinate with the solute, so that the solute coordination state changes from (4,5) to (5,5) in about half of the nonequilibrium trajectories, and in roughly 10% of the trajectories, the coordinate state can further change to (6,5). The additional solvation energy that accompanies higher-coordinated complexes is what results in the additional energy drop along the COM-to-COM distance coordinate, R, following photoexcitation in the liquid versus that in the gas phase. In other words, the energy difference is the result of the solute chemical identity changing on-the-fly during the photoreaction, effectively converting the system from a (4,5) to a (5,5) surface that has a lower zero of energy.

In summary, we performed nonequilibrium excited-state simulations via MQC MD that show that viewing moderately interacting solvent molecules as a part of the chemical identity of the solute is important to understand simple photoexcitation reactions in solution. The simulations show that the solvent plays an intimate role in the breaking of solution-phase chemical bonds. For our reaction of interest, it is clear that what originated as a photodissociation reaction of Na_2^+ in the gas phase is better understood as a two-step, sequential process of a solvated (4,5) complex, with the first step being a

https://doi.org/10.1021/acs.jpclett.2c01955
J. Phys. Chem. Lett. 2022, 13, 7931−7938

photoisomerization reaction that must be completed before the second, weakly dissociative step can take place.

We close by noting that it certainly should be possible to experimentally detect the solvent effects described above. In previous work, we argued that one could create $Na_2(THF)_n^+$ species either in mass-selected gas-phase clusters or via pulse radiolysis in solution and that the different complexes present at equilibrium could be separated by transient hole-burning.[31] Since the photoisomerization step involves rotation of the transition dipole between ground and excited state of the complex, one should be able to use polarized transient absorption spectroscopy to directly observe the isomerization reaction. This would allow direct interrogation of the role of the solvent in chemical bond breaking reactions in solution. We also expect that the solvent effects on chemical identity described above will apply generally to bond breaking and bond formation reactions in solution.

METHODS

Overview of Simulation Details. In the MQC MD simulations, the Na^+ cores and the THF solvent molecules are treated classically while the bonding electron of the solute is treated quantum mechanically. The quantum mechanical electron is treated on a basis of 64^3 grid points that span the entire simulation box. The time-independent Schrödinger equation is solved for the bonding electron at each time step. Interactions between the electron−Na^+ core and electron−THF solvent molecules are treated using pseudopotentials that have been previously developed and thoroughly benchmarked.[34−37] The quantum electron contribution to the dynamics is accounted for through the Hellman−Feynman force.

The system is composed of two Na^+ cations bound by a single quantum mechanical electron and 254 THF solvent molecules (in the liquid phase). The box size is 32.5^3 cubic angstroms to match the experimental density of THF (0.89 g/mL at ∼298 K) with periodic boundary conditions. A time step of 4 fs was used with the velocity Verlet algorithm to propagate dynamics, and all simulations were performed on the (N, V, E) ensemble at ∼298 K.

All data presented in this work are from a set of 20 adiabatic nonequilibrium trajectories for each stable Na_2^+/THF complex, (4,5) and (5,5), both in liquid THF and as gas-phase clusters. The trajectories start with uncorrelated equilibrium configurations, and at time zero, the bonding electron is promoted into the first electronic excited state, initiating nonequilibrium photodissociation dynamics. For trajectories in the liquid phase, the simulations were run for a total of 5 ps and trajectories for the gas-phase clusters were run for 3 ps. The figures presented focus on the first picosecond after photoexciation to highlight the isomerization step while including part of the dissociative step.

Molecular Geometry Coordinate. We analyzed the dynamics of our solvated complexes using a molecular geometry order parameter, h, based on the interior angles ($\angle O_{THF}$−Na^+−O_{THF}) of the solute−solvent complex. We start by defining the sum of the squares of the angle deviations from an "ideal" geometry as $\phi(t)$:

$$\phi(t) = \sum_i (\theta_i(t) - \alpha_i)^2 \tag{1}$$

where θ is the angle for the solvent configuration at time t, α is the angle of the ideal final structure (either 109.5° for tetrahedral or 90° or 120° for a trigonal bipyramidal structure), and i iterates through all interior angles of the solute−solvent complex. With $\phi(t)$ in hand, we then define our solvent geometry order parameter $h(t)$ by applying a logistic function to classify the configurations:

$$h(t) = \frac{1}{1 + \exp\left[\kappa\left(\phi(t) - \frac{1}{2}\sum_i (\alpha_i - \beta_i)^2\right)\right]} \tag{2}$$

where β_i is one of the ideal angles for either the seesaw or square pyramid initial geometry and κ is a scaling parameter, with $\kappa^{-1} = 714$ degrees^2 for seesaw to tetrahedral and $\kappa^{-1} = 570$ degrees^2 for square pyramid to trigonal bipyramid geometries. With this definition, $h(t)$ has a value of 0 when the local geometry is seesaw on the 4-coordinate side and square pyramid on the 5-coordinate side, and a value of 1 for the corresponding tetrahedral and trigonal bipyramid geometries. The values of $h(t)$ shown in Figures 2 and 3 result from averaging across both ends of the molecule.

Energy Surfaces. The blue shaded energy surfaces in Figure 3 are sampled using the enthalpy of the solute−solvent complex during the nonequilibrium dynamics. They are constructed by taking the sum of the Na^+−Na^+, Na^+−THF, and THF−THF classical potential energies and the energy of the quantum mechanical bonding electron, effectively giving us the enthalpy of the solute−solvent complex. At each 4 fs time step in our nonequilibrium ensemble, the molecular geometry, h, and photofragment distance, R, were binned with the enthalpy to create our 2-D energy surfaces. The number of values in each bin depends on how often our nonequilibrium ensemble visits each (h, R) pair. For the initial motion along the h-coordinate, i.e., along the isomerization step, there are, on average, 31 samples per bin, and for subsequent motion along the R-coordinate, i.e., the weakly dissociative step, there are, on average, 121 samples per bin. The orange curve is the ensemble average (in other words the time average) of the 20 nonequilibrium trajectories.

Coordination Number Coordinate. For determining whether or not a THF molecule is part of the solute complex, we define a continuous coordination number, n_{Na^+}, as

$$n_{Na^+} = \sum_i S(|r_{O,i} - r_{Na^+}|) \tag{3}$$

where i runs over every THF oxygen site and r_{Na^+} and $r_{O,i}$ are the positions of the Na^+ core and the ith oxygen site, respectively. We then define a counting function, $S(r)$, as

$$S(r) = \frac{1}{1 + \exp[\kappa(r - r_c)]} \tag{4}$$

where r_c is a cutoff radius that determines when a solvent molecule is coordinated to the Na^+ and κ^{-1} is the width of the transition region where the function switches from 1 to 0 around r_c. For this work, we selected $\kappa^{-1} = 0.2$ Å and $r_c = 3.65$ Å, corresponding to the first minimum of the Na^+−THF oxygen site $g(r)$. These values are similar to those used by our group in previous publications[21,30,31,37] but have been slightly reoptimized to better represent the complexation of the Na_2^+ molecule.

ASSOCIATED CONTENT

Supporting Information

The Supporting Information is available free of charge at https://pubs.acs.org/doi/10.1021/acs.jpclett.2c01955.

https://doi.org/10.1021/acs.jpclett.2c01955
J. Phys. Chem. Lett. 2022, 13, 7931−7938

Simulation details and additional data (PDF)

Photoinduced bond breaking of Na_2^+ in the gas phase (MP4)

Photoinduced bond breaking of Na_2^+ in liquid THF (MP4)

AUTHOR INFORMATION

Corresponding Author

Benjamin J. Schwartz − *Department of Chemistry & Biochemistry, University of California, Los Angeles, Los Angeles, California 90095-1569, United States;* orcid.org/0000-0003-3257-9152; Phone: (310) 206-4113; Email: schwartz@chem.ucla.edu

Authors

Andy Vong − *Department of Chemistry & Biochemistry, University of California, Los Angeles, Los Angeles, California 90095-1569, United States*

Kenneth J. Mei − *Department of Chemistry & Biochemistry, University of California, Los Angeles, Los Angeles, California 90095-1569, United States*

Devon R. Widmer − *Department of Chemistry & Biochemistry, University of California, Los Angeles, Los Angeles, California 90095-1569, United States*

Complete contact information is available at: https://pubs.acs.org/10.1021/acs.jpclett.2c01955

Author Contributions

A.V. and K.J.M contributed equally to this paper.

Notes

The authors declare no competing financial interest.

Any data generated and analyzed for this study that are not included in this Letter and its Supporting Information are available from the authors upon reasonable request. The computer code used in this study is available from the authors upon reasonable request.

ACKNOWLEDGMENTS

This work was supported by the U.S. Department of Energy Condensed Phase and Interfacial Molecular Science program under Grant No. DOE-CPIMS-0000228903. We gratefully acknowledge the Institute for Digital Research and Education (IDRE) at UCLA for use of the Hoffman2 computing cluster.

REFERENCES

(1) Young, R. M.; Neumark, D. M. Dynamics of Solvated Electrons in Clusters. *Chem. Rev.* **2012**, *112*, 5553−5577.

(2) Blandamer, M. J.; Fox, M. F. Theory and Applications of Charge-Transfer-to-Solvent Spectra. *Chem. Rev.* **1970**, *70*, 59−93.

(3) Mak, C. C.; Peslherbe, G. H. Relaxation Pathways of Photoexcited Iodide-Methanol Clusters: A Computational Investigation. *J. Phys. Chem. A* **2014**, *118*, 4494−4501.

(4) Marcus, R. A. On the Theory of Oxidation-Reduction Reactions Involving Electron Transfer. *J. Chem. Phys.* **1956**, *24*, 966−978.

(5) Marcus, R. A.; Sutin, N. Electron Transfers in Chemistry and Biology. *Biochim. Biophys. Acta* **1985**, *811*, 265−322.

(6) Barthel, E. R.; Martini, I. B.; Schwartz, B. J. How Does the Solvent Control Electron Transfer? Experimental and Theoretical Studies of the Simplest Charge Transfer Reaction. *J. Phys. Chem. B* **2001**, *105*, 12230−12241.

(7) Tran-Thi, T. H.; Prayer, C.; Millie, P.; Uznanski, P.; Hynes, J. T. Substituent and Solvent Effects on the Nature of the Transitions of Pyrenol and Pyranine. Identification of an Intermediate in the Excited-State Proton-Transfer Reaction. *J. Phys. Chem. A* **2002**, *106*, 2244−2255.

(8) Mak, C. C.; Timerghazin, Q. K.; Peslherbe, G. H. Photoinduced Electron Transfer and Solvation Dynamics in Aqueous Clusters: Comparison of the Photoexcited Iodide-Water Pentamer and the Water Pentamer Anion. *Phys. Chem. Chem. Phys.* **2012**, *14*, 6257−6265.

(9) Olivieri, J.-F.; Laage, D.; Hynes, J. T. A Model Electron Transfer Reaction in Confined Aqueous Solution. *ChemPhysChem* **2021**, *22*, 2247−2255.

(10) Liu, Q. L.; Wang, J. K.; Zewail, A. H. Femtosecond Dynamics of Dissociation and Recombination in Solvent Cages. *Nature* **1993**, *364*, 427−430.

(11) Wang, W. N.; Nelson, K. A.; Xiao, L.; Coker, D. F. Molecular-Dynamics Simulation Studies of Solvent Cage Effects on Photodissociation in Condensed Phases. *J. Chem. Phys.* **1994**, *101*, 9663−9671.

(12) Batista, V. S.; Coker, D. F. Nonadiabatic Molecular Dynamics Simulations of the Photofragmentation and Geminate Recombination Dynamics in Size-Selected I_2^--Ar_n Cluster Ions. *J. Chem. Phys.* **1997**, *106*, 7102−7116.

(13) Bihary, Z.; Zadoyan, R.; Karavitis, M.; Apkarian, V. A. Dynamics and the Breaking of a Driven Cage: I_2 in Solid Ar. *J. Chem. Phys.* **2004**, *120*, 7576−7589.

(14) Douady, J.; Jacquet, E.; Giglio, E.; Zanuttini, D.; Gervais, B. Non-adiabatic Molecular Dynamics of Excited Na_2^+ Solvated in Ar_{17} Clusters. *Chem. Phys. Lett.* **2009**, *476*, 163−167.

(15) Jonely, M.; Noriega, R. Role of Polar Protic Solvents in the Dissociation and Reactivity of Photogenerated Radical Ion Pairs. *J. Phys. Chem. B* **2020**, *124*, 3083−3089.

(16) Jonely, M.; Noriega, R. Selectively Altering the Reactivity of Transient Organic Radical Ions via Their Solvation Environment. *J. Phys. Chem. B* **2022**, *126*, 3107−3115.

(17) Kauffman, J. F. Quadrupolar Solvent Effects on Solvation and Reactivity of Solutes Dissolved in Supercritical CO_2. *J. Phys. Chem. A* **2001**, *105*, 3433−3442.

(18) Cusati, T.; Granucci, G.; Persico, M. Photodynamics and Time-Resolved Fluorescence of Azobenzene in Solution: A Mixed Quantum-Classical Simulation. *J. Am. Chem. Soc.* **2011**, *133*, 5109−5123.

(19) Sheps, L.; Miller, E. M.; Horvath, S.; Thompson, M. A.; Parson, R.; McCoy, A. B.; Lineberger, W. C. Solvent-Mediated Electron Hopping: Long-Range Charge Transfer in $IBr^-(CO_2)$ Photodissociation. *Science* **2010**, *328*, 220−224.

(20) Zanuttini, D.; Douady, J.; Jacquet, E.; Giglio, E.; Gervais, B. Nonadiabatic Molecular Dynamics of Photoexcited Li_2^+ Ne_n Clusters. *J. Chem. Phys.* **2011**, *134*, 044308.

(21) Vong, A.; Widmer, D. R.; Schwartz, B. J. Nonequilibrium Solvent Effects During Photodissociation in Liquids: Dynamical Energy Surfaces, Caging, and Chemical Identity. *J. Phys. Chem. Lett.* **2020**, *11*, 9230−9238.

(22) Ishida, T.; Rossky, P. J. Consequences of Strong Coupling Between Solvation and Electronic Strucure in the Excited State of a Betaine Dye. *J. Phys. Chem. B* **2008**, *112*, 11353−11360.

(23) Borgis, D.; Tarjus, G.; Azzouz, H. An Adiabatic Dynamical Simulation Study of the Zundel Polarization of Strongly H-bonded Complexes in Solution. *J. Chem. Phys.* **1992**, *97*, 1390.

(24) Jeanmairet, G.; Levesque, M.; Borgis, D. Tackling Solvent Effects by Coupling Electronic and Molecular Density Functional Theory. *J. Chem. Theory Comput.* **2020**, *16*, 7123−7134.

(25) Yamada, A.; Kojima, H.; Okazaki, S. A Molecular Dynamics Study of Intramolecular Proton Transfer Reaction of Malonaldehyde in Solutions Based Upon Mixed Quantum-Classical Approximation. I. Proton Transfer Reaction in Water. *J. Chem. Phys. 084509* **2014**, *141*, 084509.

(26) Kojima, H.; Yamada, A.; Okazaki, S. A Molecular Dynamics Study of Intramolecular Proton Transfer Reaction of Malonaldehyde in Solution Based Upon a Mixed Quantum-Classical Approximation.

II. Proton Transfer Reaction in Non-Polar Solvent. *J. Chem. Phys.* **2015**, *142*, 174502.
(27) Ladanyi, B. M.; Hynes, J. T. Transition-State Solvent Effects on Atom Transfer Rates in Solution. *J. Am. Chem. Soc.* **1986**, *108*, 585−593.
(28) Burghardt, I.; Hynes, J. T. Excited-State Charge Transfer at a Conical Intersection: Effects of an Environment. *J. Phys. Chem. A* **2006**, *110*, 11411−11423.
(29) Glover, W. J.; Larsen, R. E.; Schwartz, B. J. How Does a Solvent Affect Chemical Bonds? Mixed Quantum/Classical Simulations with a Full CI Treatment of the Bonding Electrons. *J. Phys. Chem. Lett.* **2010**, *1*, 165−169.
(30) Widmer, D. R.; Schwartz, B. J. Solvents Can Control Solute Molecular Identity. *Nat. Chem.* **2018**, *10*, 910−916.
(31) Widmer, D. R.; Schwartz, B. J. The Role of the Solvent in the Condensed-Phase Dynamics and Identity of Chemical Bonds: The Case of the Sodium Dimer Cation in THF. *J. Phys. Chem. B* **2020**, *124*, 6603−6616.
(32) Kahros, A.; Schwartz, B. J. Going Beyond the Frozen Core Approximation: Development of Coordinate-Dependent Pseudopotentials and Application to Na_2^+. *J. Chem. Phys.* **2013**, *138*, 054110.
(33) Szaz, L. *Pseudopotential Theory of Atoms and Molecules*; Wiley: New York, 1985.
(34) Glover, W. J.; Larsen, R. E.; Schwartz, B. J. The Roles of Electronic Exchange and Correlation in Charge-Transfer-to-Solvent Dynamics: Many-Electron Nonadiabatic Mixed Quantum/Classical Simulations of Photoexcited Sodium Anions in the Condensed Phase. *J. Chem. Phys.* **2008**, *129*, 164505.
(35) Smallwood, C. J.; Mejia, C. N.; Glover, W. G.; Larsen, R. E.; Schwartz, B. J. A Computationally Efficient Exact Pseudopotential Method. 2. Application to the Molecular Pseudopotential of an Excess Electron Interacting with Tetrahydrofuran (THF). *J. Chem. Phys.* **2006**, *125*, 074103.
(36) Glover, W. J.; Larsen, R. E.; Schwartz, B. J. First Principles Multi-Electron Mixed Quantum/Classical Simulations in the Condensed Phase. I. An Efficient Fourier-Grid Method for Solving the Many-Electron Problem. *J. Chem. Phys.* **2010**, *132*, 144101.
(37) Glover, W. J.; Larsen, R. E.; Schwartz, B. J. The Nature of Sodium Atoms/$(Na^+$-$e^-)$ Contact Pairs in Liquid Tetrahydrofuran. *J. Phys. Chem. B* **2010**, *114*, 11535−115439.
(38) Glover, W. J.; Larsen, R. E.; Schwartz, B. J. Simulating the Formation of Sodium:Electron Tight-Contact Pairs: Watching the Solvation of Atoms in Liquids One Molecule at a Time. *J. Phys. Chem. A* **2011**, *115*, 5887−5894.
(39) Vong, A.; Schwartz, B. J. Bond-Breaking Reactions Encounter Distinct Solvent Environments Causing Breakdown of Linear Response. *J. Phys. Chem. Lett.* **2022**, *13*, 6783−6791.
(40) Douady, J.; Jacquet, E.; Giglio, E.; Zanuttini, D.; Gervais, B. Solvation of Na_2^+ in Ar_n clusters. I. Structures and spectroscopic properties. *J. Chem. Phys.* **2008**, *129*, 184303.
(41) Geissler, P. L.; Chandler, D. Importance Sampling and Theory of Nonequilibrium Solvation Dynamics in Water. *J. Chem. Phys.* **2000**, *113*, 9759−9765.
(42) Dellago, C.; Bolhuis, P. G.; Csajka, F. S.; Chandler, D. Transition Path Sampling and the Calculation of Rate Constants. *J. Chem. Phys.* **1998**, *108*, 1964−1977.
(43) Bolhuis, P. G.; Dellago, C.; Chandler, D. Sampling Ensembles of Deterministic Transition Pathways. *Faraday Discuss.* **1998**, *110*, 421−436.

https://doi.org/10.1021/acs.jpclett.2c01955
J. Phys. Chem. Lett. 2022, 13, 7931−7938